M. Salehi[1]
Department of Mechanical Engineering,
Institute for Information Management
in Engineering,
Karlsruhe Institute of Technology,
Kaiserstr. 12,
Karlsruhe 76131, Germany;
Department of Mechanical Engineering
and Mechatronic,
Institute of Materials and Processes,
Karlsruhe University of Applied Science,
Moltkestr.30,
Karlsruhe 76133, Germany
e-mail: mehdi.salehi@hs-karlsruhe.de

T. L. Schmitz
Department of Mechanical Engineering and
Engineering Science,
University of North Carolina at Charlotte,
Charlotte, NC 28223

R. Copenhaver
Department of Mechanical Engineering and
Engineering Science,
University of North Carolina at Charlotte,
Charlotte, NC 28223

R. Haas
Department of Mechanical Engineering
and Mechatronic,
Institute of Materials and Processes,
Karlsruhe University of Applied Science,
Moltkestr.30,
Karlsruhe 76133, Germany

J. Ovtcharova
Department of Mechanical Engineering,
Institute for Information Management in
Engineering,
Karlsruhe Institute of Technology,
Kaiserstr. 12,
Karlsruhe 76131, Germany

Probabilistic Sequential Prediction of Cutting Force Using Kienzle Model in Orthogonal Turning Process

Probabilistic sequential prediction of cutting forces is performed applying Bayesian inference to Kienzle force model. The model uncertainties are quantified using the Metropolis algorithm of the Markov chain Monte Carlo (MCMC) approach. Prior probabilities are established and posteriors of the models parameters and force predictions are completed using the results of orthogonal turning experiments. Two types of tools with chamfer (rake) angles of 0 deg and −10 deg are tested under various cutting speed and feed per revolution values. First, Bayesian inference is applied to two force models, Merchant and Kienzle, to investigate the cutting force prediction at the low feed values for the 0 deg rake angle tool. Second, the results of the posteriors of the Kienzle model parameters are used as prior probabilities of the −10 deg rake angle tool. The simulation results of the 0 deg and −10 deg tool rake angle are compared with the experiments which are obtained under other cutting conditions for model verification. Maximum prediction errors of 7% and 9% are reported for the tangential and feed forces, respectively. This indicates a good capability of the Bayesian inference for model parameter identification and cutting force prediction considering the inherent uncertainty and minimum input experimental data. [DOI: 10.1115/1.4041710]

Keywords: machining, cutting force, Kienzle model, Bayesian inference, MCMC

1 Introduction

Machining models provide relationships between user-selected inputs (feed, cutting speed, tool geometry) and the process outputs, such as cutting forces. The models may be numerical or analytical in format. In this context, several models have been proposed [1–4] to predict cutting forces in milling and turning operations. In general, machining models are deterministic. In other words, given a set of inputs, a unique set of outputs is obtained. However, to establish a predictive model, the mean and distribution in the outputs must be related to the input means and distributions. This probabilistic approach incorporates the inherence uncertainties. These uncertainties are due to the machine and machining process, workpiece material, measurement process, tool material, and tool geometry, among others. The uncertainty evaluation and probabilistic modeling of the machining process can be performed by Bayesian inference [5]. Karandikar et al. [6,7] investigated application of grid-based and Bayesian Markov chain Monte Carlo (MCMC) to predict the tool life in milling and turning processes. The grid-based method was used for inference on Taylor tool life model parameters, whereas the Metropolis MCMC was applied to estimate the extended Taylor's model parameters. The performance comparison of two approaches was also reported, where the grid-based method was easier to implement, but it was computationally more expensive for updating a joint distribution with three or more dimensions. On the other hand, the Metropolis algorithm facilitated sampling from multivariate distributions without sensitivity to the number of the parameters [8]. Niaki et al. [9,10] developed probabilistic models using Bayesian inference to predict tool wear in milling of Nickel-based material. The combined Gibbs-Metropolis algorithm was used to estimate the unknown parameters of a nonlinear mechanistic cutting power model. The Metropolis algorithm was used for predicting the model parameters, whereas the Gibbs sampler was utilized for updating measurement error variance. By using the algorithm, the model parameters were successfully estimated with the maximum error of 18%.

Gözü and Karpat [11] studied application of Bayesian inference to predict cutting force in micromilling of Titanium alloy TiAl4V. The Metropolis–Hasting algorithm of MCMC was used to identify probability distributions of the cutting and ploughing forces coefficients based on experimental measurements and a mechanistic model of micromilling. The mechanistic model can predict the cutting and ploughing forces in radial and tangential directions,

[1]Corresponding author.

Manuscript received June 4, 2018; final manuscript received October 4, 2018; published online November 8, 2018. Assoc. Editor: Laine Mears.

where the cutting forces are linearly proportional to the uncut chip thickness. Schmitz et al. [12] investigated cutting force prediction under uncertainty using Bayesian inference for the Merchant model, where the cutting force is linearly proportional to the feed-dependent uncut chip thickness. Discrete grid method was used to update the force model parameters. Mehta et al. [13] developed a mechanistic force model for cutting force prediction using MCMC approach again applied to the Merchant model. The force models, which have been used in the above-mentioned papers, describe linear relationships between the cutting and ploughing forces and the feed values. Nevertheless, the probabilistic cutting force prediction considering the "size effect" phenomenon is yet to be investigated using nonlinear models such as Kienzle force model [14]. The term size effect refers to as the nonlinear increase of the specific cutting energy with decreasing the undeformed chip thickness. A good summary of the phenomenon and the modeling techniques are given by Vollertsen et al. [15].

In this paper, Bayesian inference is applied to the Merchant and Kienzle force models to predict the cutting forces at very low feed values in turning. Metropolis algorithm of the MCMC method is used to estimate the force models' parameters. In order to investigate the effect of cutting tool geometry on cutting forces, two cutting tool rake angles, 0 deg and −10 deg, are tested under different cutting conditions in an orthogonal turning process. First, the probabilistic prediction of tangential force using the Merchant model for the 0 deg rake angle tool is presented. Next, Bayesian inference is applied to the Kienzle model to predict tangential and feed forces for the 0 deg and −10 deg rake angle tools, sequentially.

This paper is organized as follows: in Sec. 2, deterministic Merchant and Kienzle cutting force models are presented. In Sec. 3, the experimental setup and the measurement results are illustrated. In Sec. 4, the Bayesian inference scheme and MCMC method are presented. In Sec. 5, the application of MCMC to the Merchant and Kienzle force models using the 0 deg tool rake angle is presented and discussed. The results of the posterior forces and parameters of the Kienzle model for the 0 deg rake angle tool are used to predict forces for the −10 deg rake angle tool in Sec. 6. Conclusions are provided in Sec. 7.

2 Cutting Force Models

Deterministic models of the Merchant and Kienzle force models are presented in this section. The Mechanistic Merchant model is based on an assumption that the tool edge radius is zero. However, Kienzle force model takes into account the effect of cutting edge radius on specific cutting force coefficient. Weber et al. [14] investigated increase of the force coefficients comparing two edge radii of 5 and 50 μm, where the larger cutting edge radius resulted in a higher specific cutting force. They also reported that the edge radius of the tool used in the investigations to derive the Kienzle equation was probably in the range of 10–20 μm.

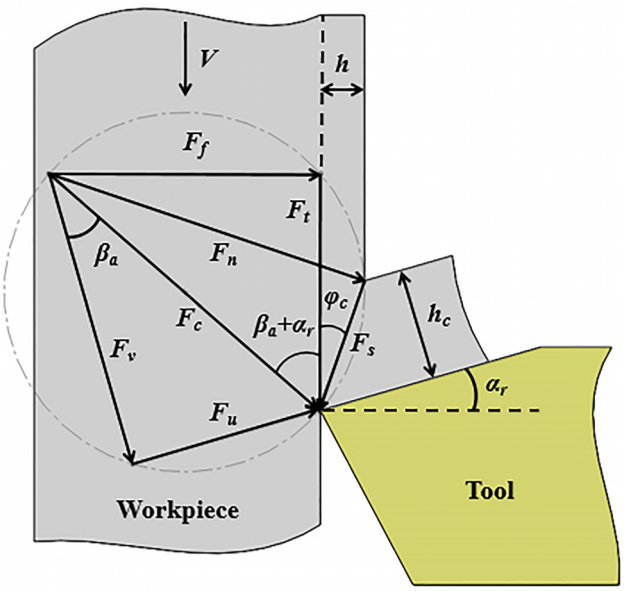

Fig. 1 Merchant cutting force diagram

2.1 Merchant Force Model. Merchant force model describes linear relationships between cutting force and the uncut chip thickness, h [16]. Figure 1 displays a schematic orthogonal cutting model for the cutting forces calculation. According to the figure, the tangential force, F_t, is calculated as follows:

$$F_t = K_t b h \tag{1}$$

where K_t is the tangential cutting force coefficient, b is the width of cut, and h is the uncut chip thickness. The width of the cut and the feed value are decided by the machinist, while the cutting force coefficient must be calculated. In order to calculate F_t, one needs to find K_t as follows:

$$K_t = \tau_s \frac{\cos(\beta_a - \alpha_r)}{\sin(\phi_c)\cos(\phi_c + \beta_a - \alpha_r)} \tag{2}$$

where τ_s is the shear stress along the shear plane, ϕ_c is the shear plane angle, β_a is the average friction angle, and α_r is the tool rake angle. The τ_s is determined as following:

$$\tau_s = \frac{F_s}{A_s} \tag{3}$$

where F_s is the shear force, and A_s is the shear area. The β_a is obtained as follows:

$$\beta_a = \alpha_r + \tan^{-1}\left(\frac{F_f}{F_t}\right) \tag{4}$$

The shear plane angle, ϕ_c, can be obtained by measuring the cut chip thickness, as follows:

$$\phi_c = \tan^{-1}\left(\frac{r_c \cos(\alpha_r)}{1 - r_c \sin(\alpha_r)}\right) \tag{5}$$

$$r_c = \frac{h}{h_c} \tag{6}$$

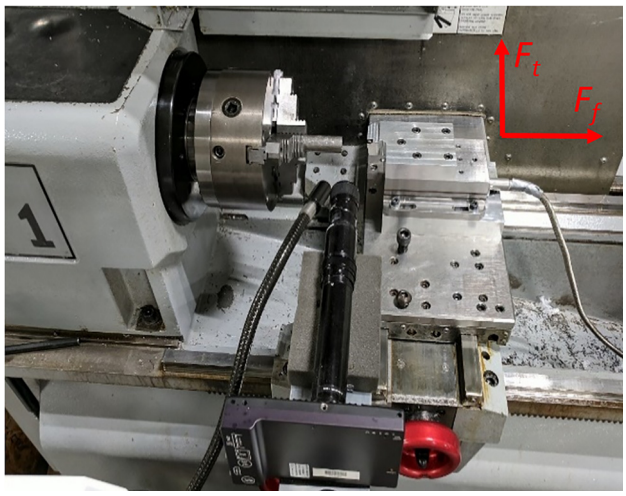

Fig. 2 Machining experiments setup and the cutting forces directions

where h_c is the cut chip thickness and r_c is the chip thickness ratio.

2.2 Kienzle Force Model. The Kienzle force model describes a nonlinear relationship between h and the cutting force components in the tangential and feed directions, F_t and F_f, respectively [17]

$$F_t = K_{tt}.b.h^{1-c_t} \tag{7}$$

$$F_f = K_{ff}.b.h^{1-c_f} \tag{8}$$

where the 1-c_t and 1-c_f exponents are positive constants less than one, and K_{tt} and K_{ff} are the tangential and feed cutting force coefficients. The force coefficients depend on the workpiece material, and the exponents depend on the geometrical cutting parameters, cutting speed, and the tool-workpiece combination.

3 Experimental Setup and Results

Tube turning (orthogonal cutting) experiments were performed on a Haas TL-1 CNC lathe; see Fig. 2. The dry machining tests were completed using a Kennametal turning insert, CCMW3252, with 0 deg rake angle as well as uncoated inserts SPGW09T308 with the rake angle −10 deg and the edge radius of 20 μm. The latter insert was designed and produced with the special edge geometry by Zermet Zerspanung GmbH with the ISO grade of P25.

The tubular workpiece material was AISI 1020 steel with an outer diameter of 25.4 mm and wall thickness of 2.1 mm. The corresponding chip width was 2.1 mm. Feed values of $h = \{0.051, 0.076, \text{ and } 0.102\}$ mm/rev, as well as three cutting speeds of $V_c = \{60, 80, \text{ and} 100\}$ m/min were selected. The experiments were repeated three times for each cutting speed-feed combination. Therefore, the total number of experiments was 54. A three-axis force dynamometer (Kistler 9257B) was used to measure the cutting forces in the tangential and feed directions. For both tool geometries, one to two data sets were used to update the probabilistic models, while the others were used for the probabilistic model verification.

3.1 Results of the Cutting Force and Chip Thickness Measurement. Twelve tangential and feed forces were selected for training of the Merchant and Kienzle model parameters. Figures 3 and 4 display the tangential and feed force data under different cutting conditions using the two tool geometries (0 and −10 deg rake angles). The mean is provided together with one standard deviation error bars. As expected, the forces increase with the increase of feed for the both geometries. One interesting observation is that the tangential force component is larger for the 0 deg rake tool, while the feed component is larger for the −10 deg rake tool.

Figure 5 shows the mean and one standard deviation of cut chip thickness values, which were measured by a dial caliper along the machined chips. The values are used to train the prior of the merchant model parameters for the 0 deg rake angle tool. According to the figure, the cut chip thickness values increase with an increase in feed values.

4 Bayesian Inference

Bayesian inference enables the prior or initial belief about a parameter, to be updated by new experimental results. In Bayesian inference, a probability represents a degree of belief. According to Eq. (9), the posterior probability, $p(x/y)$, which represents new beliefs after new information is obtained, is calculated by multiplying the prior, $p(x)$, by the likelihood function $p(y/x)$ and dividing by the normalizing function. Using the Bayesian approach, the posterior distribution of the one study can be used as the prior distribution of a second study

$$p(x|y) = \frac{p(x)p(y|x)}{\int p(x)p(y|x)dx} \tag{9}$$

The integral in Eq. (9) is often referred to as the marginal probability and generally does not have a closed-form solution. Therefore, various computational approaches have been developed to supplement or replace analytical integration to determine the posterior distribution. One popular numerical approach is the MCMC algorithm [18]. This algorithm has played a significant role in machine learning, statistics, econometrics, physics, and decision analysis over the last two decades.

4.1 Markov Chain Monte Carlo Approach. The MCMC method is a sampling technique used to draw sample from a probability density function (PDF). Random samples, x, are generated using a Markov chain mechanism to approximate a distribution of interest, which is often called target distribution, $p(x)$. Among the different MCMC methods, the Metropolis–Hastings (MH) algorithm is the most popular. The MH technique can be used for drawing samples from symmetric and asymmetric proposal distributions. Metropolis algorithm is a special case of the MH algorithm, where the proposal function is symmetric. A normal distribution is often used as a symmetric proposal PDF denoted as $q(x)$. A candidate sample, x_{new}, drawn from the proposal

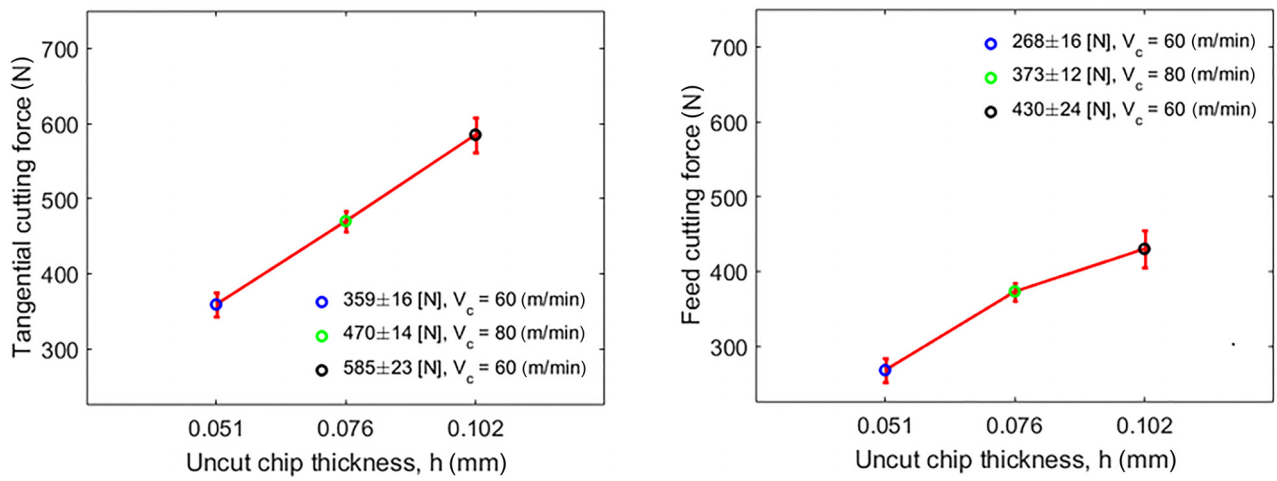

Fig. 3 Tangential and feed force components for training of the priors using tool rake angle 0 deg

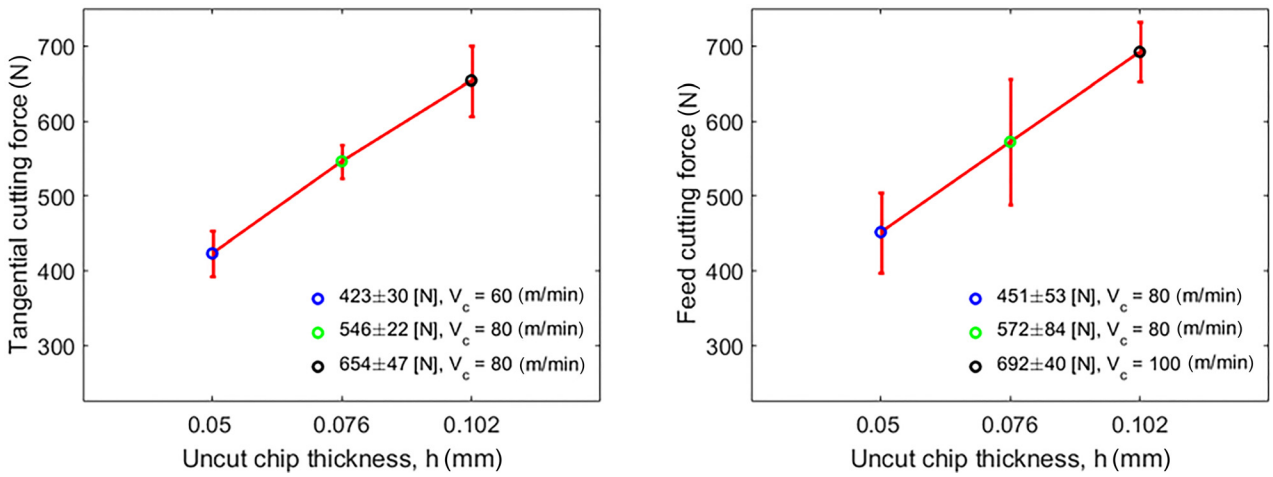

Fig. 4 Tangential and feed force components for training of the priors using tool rake angle −10 deg

distribution is either accepted or rejected depending on an acceptance ratio of the posteriors, r. In each iteration, the Markov chain moves to x_{new} if the sample is accepted. Otherwise, the chain remains at the current value of x. The algorithm proceeds for $N-1$ iterations to obtain N samples from the target distribution using the following steps [7]:

(1) Initialize a starting sample x^0,
(2) For $i = 0$ to $i = N-1$:
- Select a candidate x^{new} from a proposal distribution, $q(x^{new}/\, x^i)$,
- Calculate the acceptance ratio, $r = (p(x^{new})/P(x^i))$,
- Generate a random number, $u \sim$ *uniform* $(0,1)$,

If $u \leq r$:
Accept the proposal: $x^{i+1} = x^{new}$,
Else:
Reject the proposal: $x^i = x^{new}$,
End If

(3) End For

In order to reduce the excessive autocorrelation of the drawn samples using Metropolis algorithm, the thinning technique is used. Additionally, the proposal distribution of the samples is tuned by selecting the sample acceptance rate roughly between 25 and 45%, [19,20]. The initial iterations are typically discarded as burn-in period to reduce the effect of the initial errors at the beginning of the chain [21]. A practical way to evaluate convergence to the chain's stationary distribution is by observing the traces and histograms of the parameters [5]. To assess convergence of MCMC draws within a chain, Geweke method is used. The method proposes a convergence diagnostic for Markov chains based on comparison of the last part of the chain against some smaller interval in the beginning of the chain (e.g., the first 10% and last 50% after removing the burn-in period). If the chain is at the stationary condition, the sample means of two intervals are almost equal (e.g., the difference is less than 3%) [22].

In this paper, blockwise updating technique of the Metropolis algorithm is used to sample from bivariate probability distributions. In this method, proposal distributions are selected to have the same dimensionality as the target distributions, so that the proposal distributions are either accepted or rejected as a block.

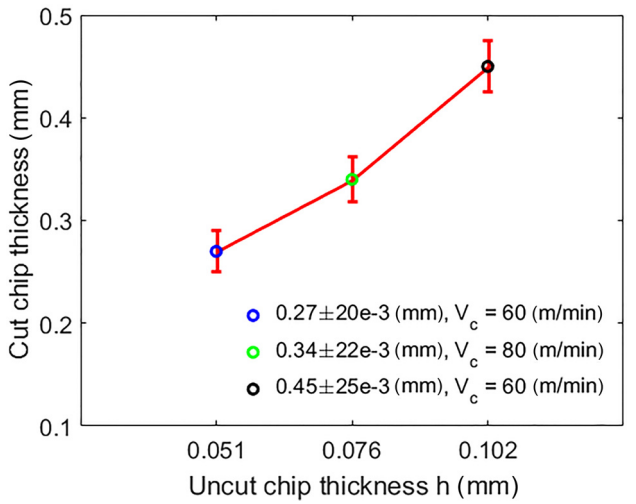

Fig. 5 Mean and one standard deviation of the cut chip thickness using the 0 deg rake angle tool

5 Application of Markov Chain Monte Carlo to Merchant and Kienzle Force Models Using Rake Angle 0 Deg Tool

Bayesian MCMC approach is applied to the Merchant force model to predict the tangential force, first. Next, MCMC approach is applied to the Kienzle force model to predict the tangential and feed forces. Summary of the steps of the MCMC application to the force models are described as following:

(1) Establishing the priors of the force models' parameters.
(2) Parameters updating using the likelihood function of the measured forces.

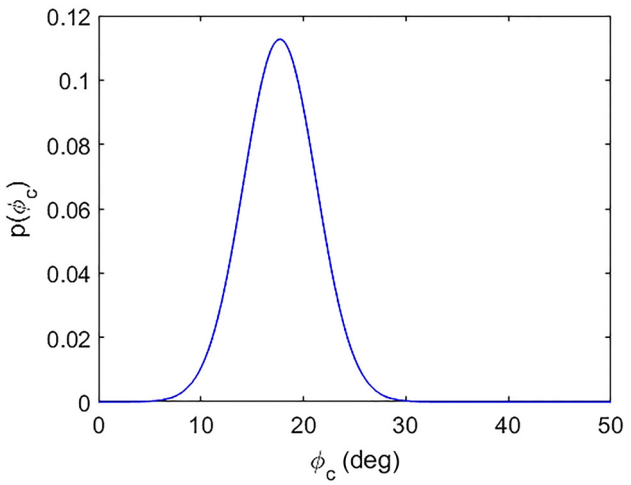

Fig. 6 Prior distribution of ϕ_c

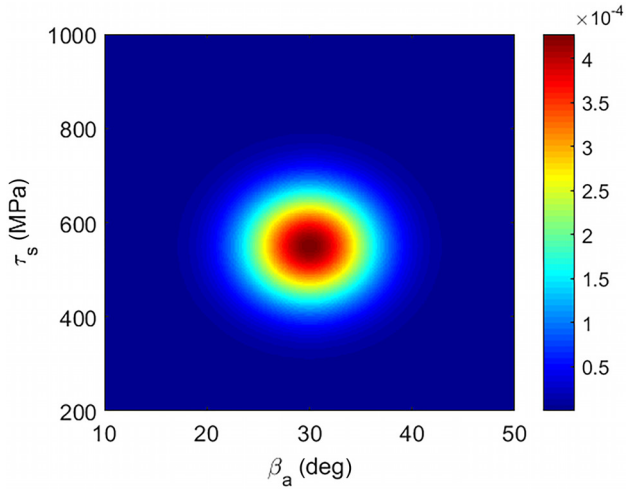

Fig. 7 Joint distribution of β_a and τ_s

(3) Computing of the posterior distribution of the force models' parameters and cutting forces using MCMC Metropolis algorithm.

5.1 Application of Markov Chain Monte Carlo to Merchant Model. In the Merchant force model, there is uncertainty in the force coefficient, K_t, due to the uncertainty in the model parameters, ϕ_c, β_a, and τ_s. The uncertainty evaluation and minimization using Bayesian MCMC are explained in this section.

5.1.1 Establishing the Priors. Prior of the model parameters were obtained from literature reviews [12]. In the literatures, the results of the cutting tests were reported for a range of tool rake angles, +5, 0, and −7 deg, the cutting speed values of 100–400 m/min and feed values of 0.1–0.5 mm/rev. The prior mean and one standard deviation values of the parameters are given as follows:

(1) $\phi_c = 17 \pm 4$ deg
(2) $\beta_a = 30 \pm 5$ deg
(3) $\tau_s = 550 \pm 80$ MPa

Figure 6 shows the normal prior distribution of ϕ_c, and Fig. 7 illustrates joint Gaussian prior distribution of β_a and τ_s, with an independent covariance matrix. Monte Carlo sampling was

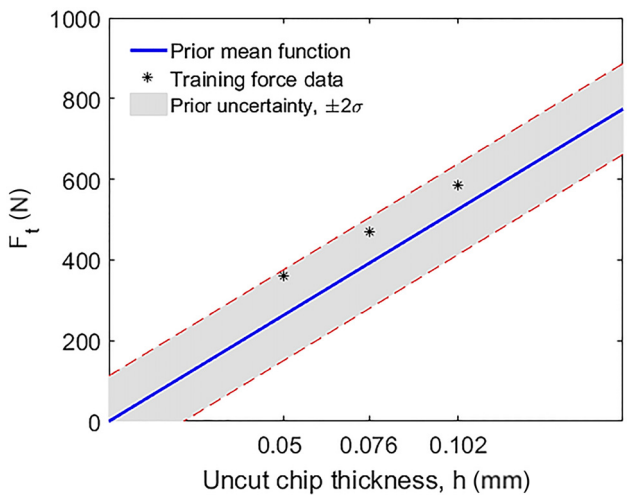

Fig. 8 Prior function of tangential cutting force with $\pm 2\sigma$ standard deviation uncertainty intervals

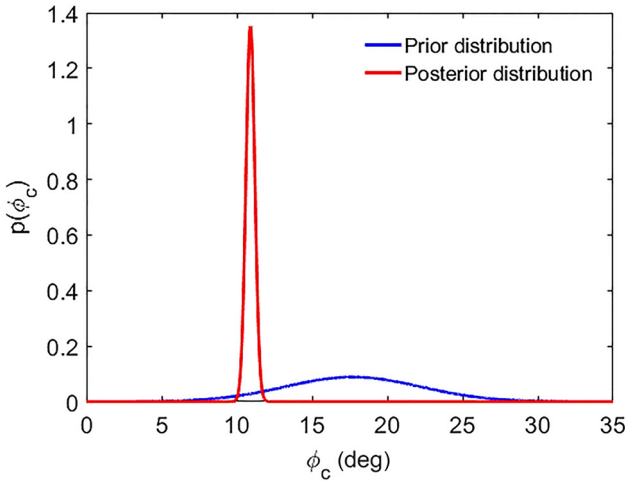

Fig. 9 Comparison of prior and posterior distributions of ϕ_c after three updates

practiced for Eq. (2) to find the distribution of tangential force coefficient, K_t. The mean and one standard deviation of K_t were computed to be 2447 and 528 MPa.

Once again, Monte Carlo simulation was used to calculate the prior for the tangential cutting force using Eq. (1). Figure 8 illustrates the functional form of the prior mean value, two standard deviation (2σ) uncertainty intervals, and the training force data points. According to the figure, the prior mean function underestimates the forces.

5.1.2 Parameters Updating. This section describes the model parameters updating using the likelihood function and Metropolis MCMC method. In this regard, first, the parameter ϕ_c is updated using the measured h_c. Next, random samples from the posterior of ϕ_c, together with the measured force values are used to update the joint PDF of the parameters β_a and τ_s [12]. Likelihood function of the shear plane angle is written as following:

$$p(\phi_c^m|\phi_c) = e^{-\frac{(\phi_c-\phi_c^m)^2}{2\sigma_{c,m}^2}} \tag{10}$$

where ϕ_c^m is the measured shear plane angle, which is calculated using measured cut chip thickness, h_c, as an input into Eqs. (5) and (6), $\sigma_{c,m}$ is the standard deviation or variation of the measured cut chip thickness, which is obtain to be 7–10% of the mean value. The likelihood is the value of the normal PDF for the measured

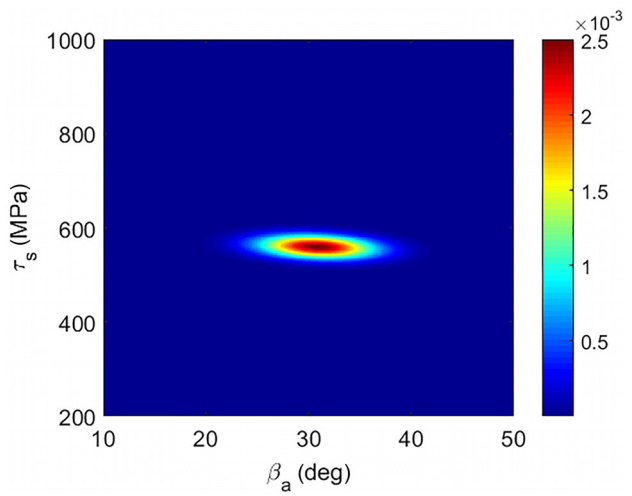

Fig. 10 Joint PDF of β_a and τ_s after three updates

shear plane angle, ϕ_c^m, given the specified values of the ϕ_c as prior. This likelihood function describes how likely the measurement result at a feed is, given force parameters priors. In other word, if the priors result in a force, which is near to the measured force, the likelihood is high; otherwise it is low.

Posterior distribution of ϕ_c was calculated by multiplying the prior of the into the likelihood function using Metropolis algorithm. In this context, $N = 10{,}000$ samples were drawn from the proposal normal distribution, $q(\phi_c)$. After removing the first 1500 points as the burn-in period, the acceptance rate of 28% was obtained. Figure 9 shows the prior and posterior distributions of ϕ_c after three updates. The posterior mean value is 10.9 deg, and the one standard uncertainty interval is minimized to 0.29 deg.

The same procedure was followed to update the joint prior distribution of (β_a,τ_s) using the measured force values and the samples from the ϕ_c posterior. Similarly, blockwise MCMC method was exercised to draw $N = 10{,}000$ samples from the joint normal proposal distribution, $q(\beta_a,\tau_s)$. After discarding of the first 1500 samples as the burn-in period, the acceptance rate of 41% was obtained. Figure 10 displays the joint posterior distributions of β_a and τ_s after three updates. The mean values of β_a and τ_s, are 30.8 deg and 559 MPa, and the standard deviations are 3.8 deg and 17 MPa, respectively.

Although, the prior joint PDF of (β_a,τ_s) were taken to be independent, the parameters become correlated after running the MCMC simulation. This can be quantified using Pearson correlation coefficient. The correlation coefficient is the measure of linear relationship between two parameters defined as the covariance of the parameters divided by the product of their standard deviations; see the following equation:

$$\rho(\beta_a, \tau_s) = \frac{\text{cov}(\beta_a, \tau_s)}{\sigma_{\beta_a}\sigma_{\tau_s}} \tag{11}$$

The correlation coefficient of the parameters, β_a and τ_s, was calculated to be -0.2. Monte Carlo simulation is used to calculate the posterior distribution of the coefficient, K_t, using the posteriors of the model parameters, ϕ_c, β_a, and τ_s, for Eq. (2). Figure 11 shows the prior and posterior distributions of K_t. The posterior mean and standard deviation values were computed to be 3408 and 135 MPa. As illustrated, the uncertainty is minimized after three updates.

5.1.3 Cutting Force Prediction. Figure 12 demonstrates the posterior function of the cutting force with two standard deviation (2σ) uncertainty intervals.

As can be seen in Fig. 12, despite of the uncertainty assignment to the posterior mean function, the Merchant model is not able to predict all the training forces within the experimental feed values. This represents the nonlinear relationship of the forces and uncut chip thickness at the low feed values. The nonlinearity can be due to the increase of the specific cutting energy with the reduced uncut chip thickness or increase of tool edge radius, so that the energy expended in shearing the chip due to the apparent more negative effective rake angle (size effect phenomenon) [23]. The size effect is often described with the Kienzle force model [14].

5.2 Application of Markov Chain Monte Carlo to Kienzle Model. Blockwise Metropolis algorithm is again used to evaluate the uncertainty of the Kienzle force model parameters and the forces prediction. The uncertainty of the tangential and feed forces, F_t and F_f, originates from the uncertainty in the model parameters K_{tt}, K_{ff}, c_t, and c_f.

5.2.1 Establishing the Prior. The parameter identification starts with establishing prior values for K_{tt}, K_{ff}, c_t, and c_f. The mean and standard deviation of the parameters were taken from Ref. [24] for a range of low carbon steel cutting operations

(1) $K_{tt} = 1620 \pm 96$ MPa
(2) $K_{ff} = 350 \pm 140$ MPa
(3) $c_t = 0.28 \pm 0.04$
(4) $c_f = 0.33 \pm 0.025$

Figure 13 shows the priors of the pairs (K_{tt},c_{tt}) and (K_{ff},c_f) using Gaussian joint distributions; the covariance matrices were taken to be independent. Moreover, the functional form of the mean values for the priors with two standard deviation uncertainty intervals are displayed in Fig. 14. The training data are also shown. According to the figure, the prior mean function of the tangential force over-estimates the training force data, while the prior mean function of the feed force underestimates it.

The bivariate likelihood function of the measured tangential force given the Kienzle force coefficients is

$$p(F_{tm}|K_{tt}, c_t) = e^{-\frac{((K_{tt}.b.h^{1-c_t})-F_{tm})^2}{2\sigma_{F_{tm}}{}^2}} \tag{12}$$

where $pv(F_{tm}/K_{tt},c_t)$ is the likelihood function of the measured tangential force mean, F_{tm}, given specified prior values of the force coefficients, (K_{tt},c_t), at an experimental feed value. The likelihood function is expressed as a non-normalized normal distribution, where σ_{Ftm} is the standard deviation of the tangential measured force. The likelihood function was also calculated for the measured feed force mean, F_{fm}, given specified prior values of the force coefficients, (K_{ff},c_f). In this study, the standard deviation of the tangential and feed forces was considered 4–6% of the measured

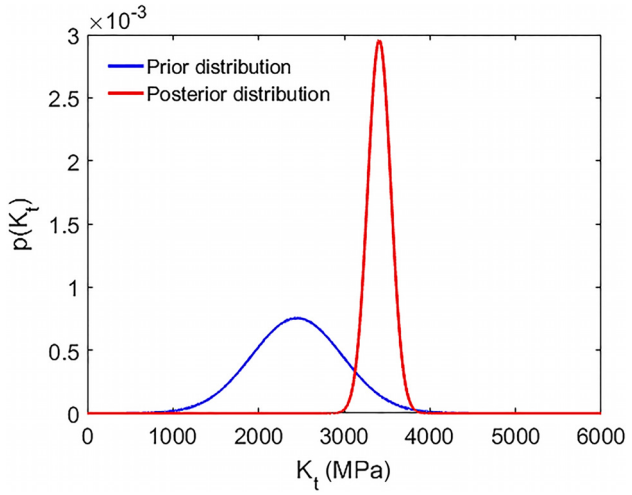

Fig. 11 Comparison of prior and posterior distributions of the K_t, after three updates

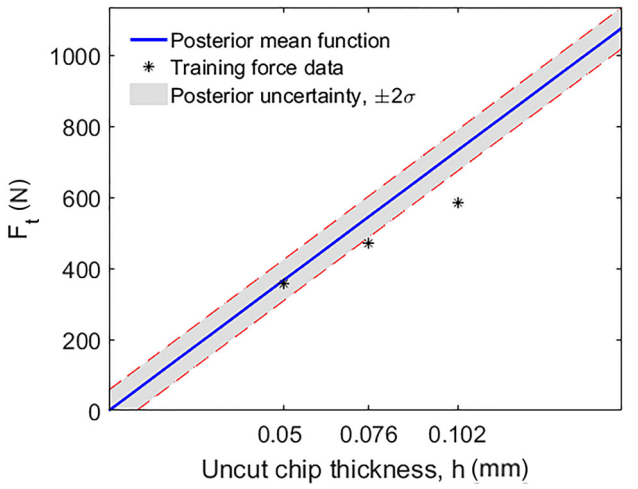

Fig. 12 Posterior function of tangential cutting force with $\pm 2\sigma$ standard deviation uncertainty intervals

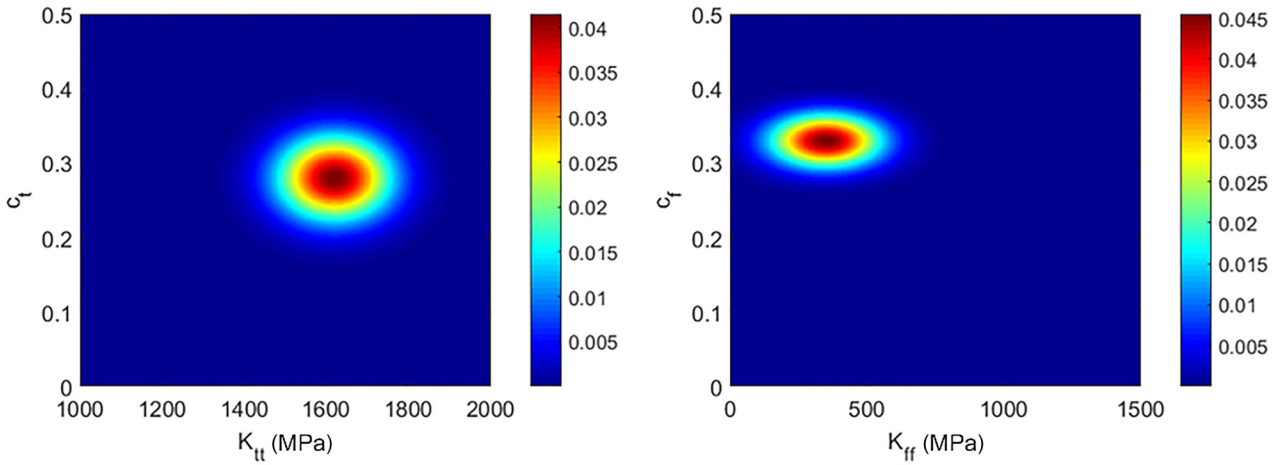

Fig. 13 Joint Gaussian prior distributions of K_{tt} and c_{tt} (left), and K_{ff} and c_f (right) for the tool rake angle 0 deg

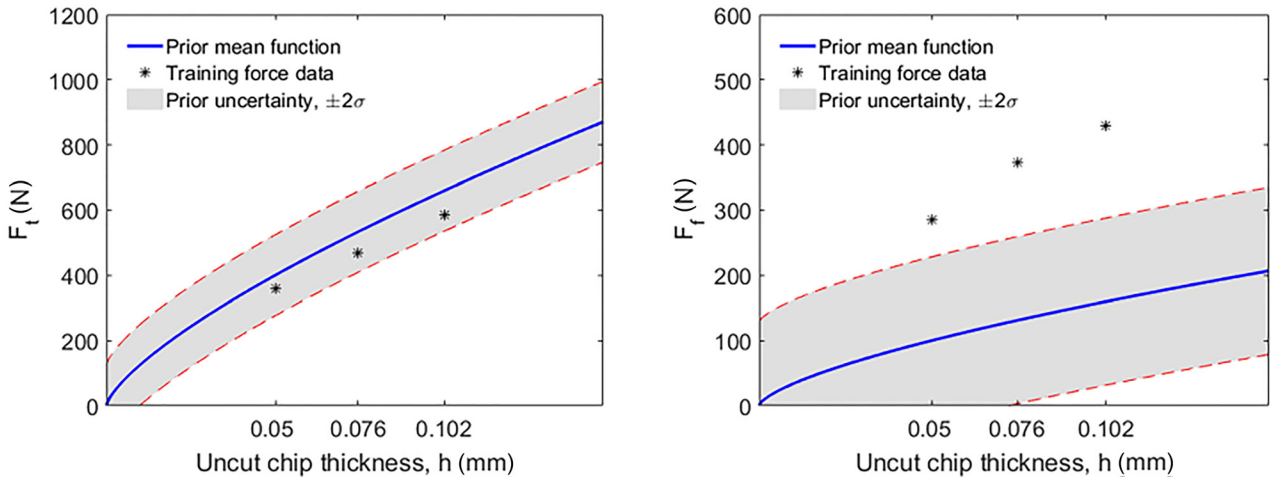

Fig. 14 Prior functions of the tangential forces (left) and feed force (right) with $\pm 2\sigma$ standard deviation uncertainty intervals for the tool rake angle 0 deg

forces mean values. Joint posterior distributions, (K_{tt},c_t) and (K_{ff},c_f), were calculated by multiplying the priors into the likelihood functions using blockwise Metropolis algorithm. $N = 10{,}000$ samples were drawn from the proposal normal distributions, $q(K_{tt},c_t)$ and $q(K_{ff},c_f)$, and 1500 samples were considered as the burn-in period. The covariance matrices of the proposal distributions were tuned, so that the acceptance rate values of 44% and 33% were obtained for the drawn samples of the tangential and feed model parameters, respectively.

Figure 15 displays the bivariate posterior distributions of K_{tt} and c_t (left), which is obtained after one update, in addition to K_{ff} and c_f (right) achieved after two updates using measured forces.

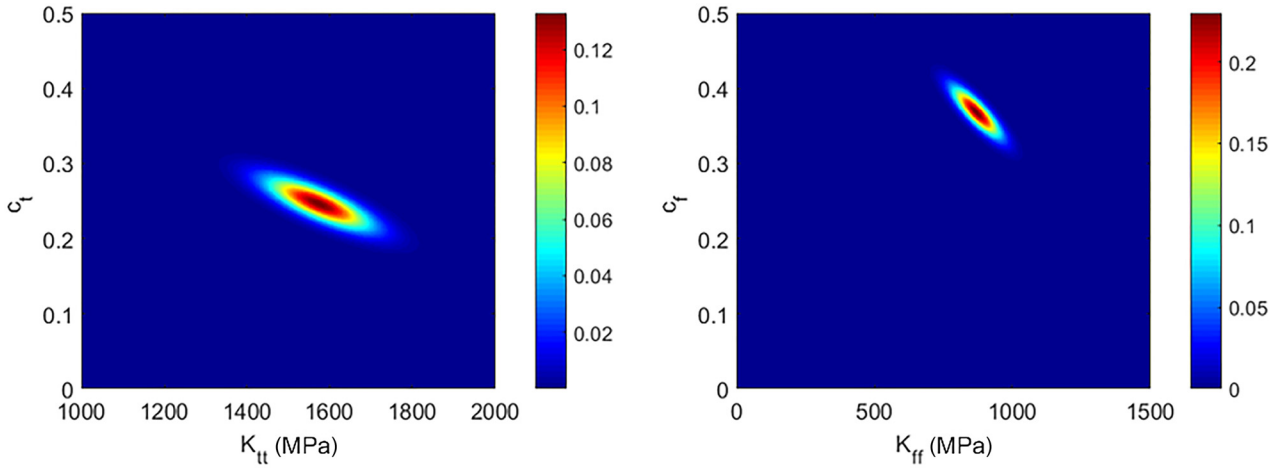

Fig. 15 Joint posterior distributions of K_{tt} and c_{tt} (left), and K_{ff} and c_f (right), for the tool rake angle 0 deg

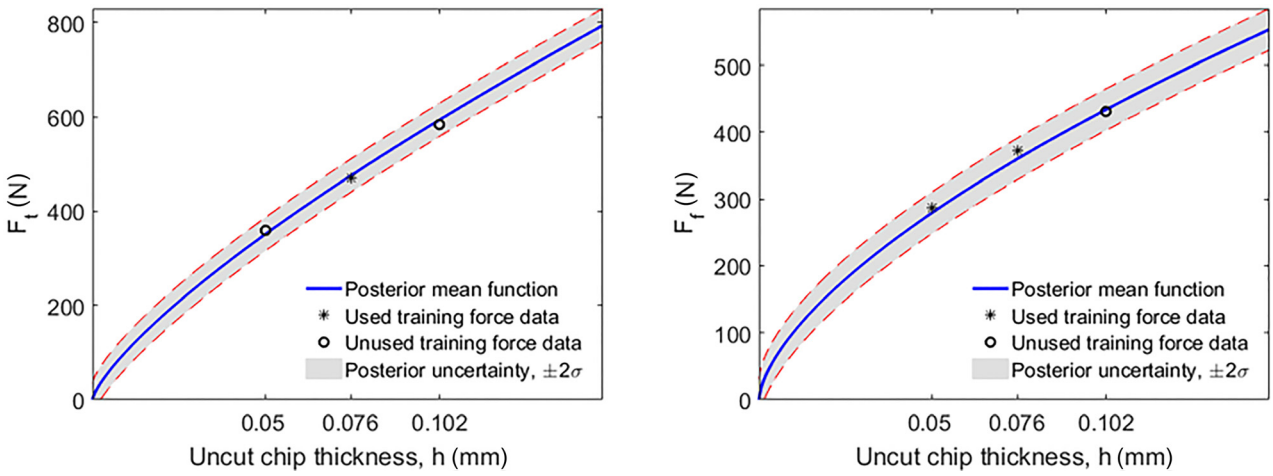

Fig. 16 Posterior functions of tangential (left) and feed (right) force with $\pm 2\sigma$ standard deviation uncertainty intervals for the tool rake angle 0 deg

For the tangential force component, the mean values of K_{tt} and c_t are computed to be 1573 MPa and 0.24, and the standard deviations are 84 MPa and 0.023, respectively. For the feed force component, the mean values of K_{ff} and c_f are 870 MPa and 0.36, and the standard deviations are 58 MPa and 0.022, respectively. Comparing the posterior and prior joint distributions, it is seen that the uncertainties are reduced. Additionally, the model parameters become correlated with the correlation coefficient of -0.78 for (K_{tt},c_t) and -0.85 for (K_{ff},c_f) joint distributions.

5.2.2 Cutting Force Prediction. Force prediction is performed using the posterior distributions of K_{tt} and c_t and K_{ff} and c_f for Eqs. (7) and (8). Figure 16 shows the functional form of the tangential and feed forces posteriors with the mean and two standard deviations. The regression fit is characterized by $R^2 = 0.99$ (tangential force), and $R^2 = 0.98$ (feed force). As can be seen, only one force is used for updating of the tangential force posterior, and two forces are used for training of the feed force posterior function. The posterior mean functions closely agree with the forces. This is due to the influence of the informative prior knowledge in the tangential direction (which leads to using of only one training force) and less informative prior in the feed direction.

Figure 17 illustrates the prediction of the cutting forces obtained under other cutting conditions. As can be seen, all the force data appear within the uncertainty intervals. Table 1 lists the experimental force values and the predicted mean with two standard deviation (2σ) uncertainty intervals of the tangential and feed forces for the 0 deg tool rake angle. Percent error between the measured and predicted mean forces is also reported in the table, where the maximum prediction error for the tangential force was calculated to be 5% and for the feed force is 8%. This indicates that the algorithms are able to identify the model parameters and predict the forces with a good degree of accuracy. Consequently, the probabilistic prediction of the forces using Kienzle model causes more accurate estimation and can capture the nonlinearity of the measured forces in both tangential and feed directions.

6 Sequential Force Prediction Using the Kienzle Force Model

Sequential force prediction is performed by using the posterior distributions of the Kienzle model parameters from the 0 deg rake tool as the prior distributions for the -10 deg rake angle tool; see Fig. 18. As illustrated in the figure, the model parameter priors are trained by 0 deg rake experiments to obtain the posterior force distributions. Next, the posterior distributions of the 0 deg rake angle tool are used as prior probabilities for the -10 deg rake angle tool. The training procedure can be continued to update and predict the forces using other rake angles as well.

6.1 Model Parameter Identification. To establish the mean and standard deviation for the priors of the new geometry (tool rake angle -10 deg), following steps were implemented:

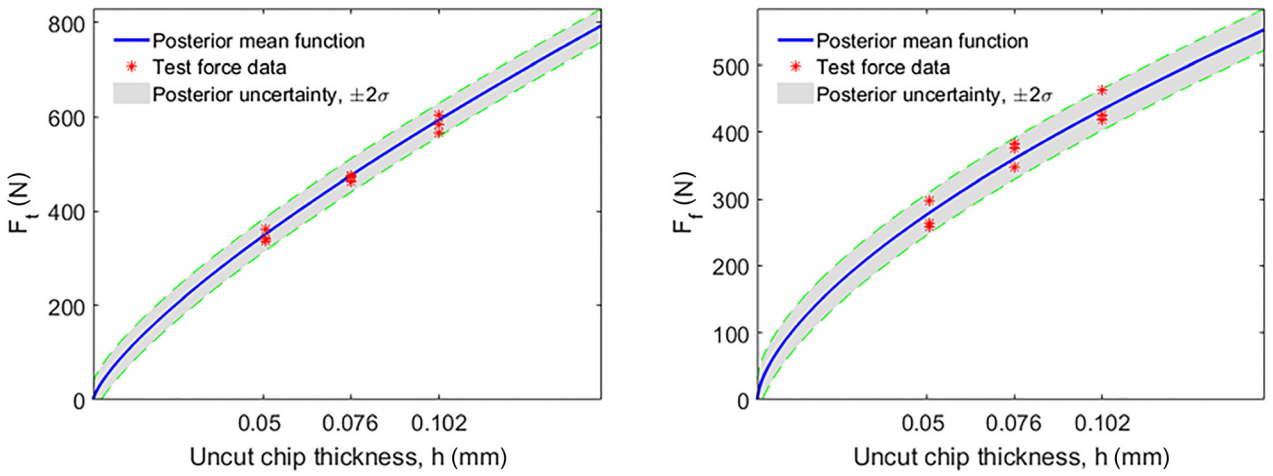

Fig. 17 Posterior functions for prediction of tangential (left) and feed (right) forces with $\pm 2\sigma$ standard deviation uncertainty intervals for the tool rake angle 0 deg

Table 1 Measured and predicted forces and the corresponding percentage error using the 0 deg tool rake angle

No.	V_c (m/min)	f (mm/rev)	$F_{t\_measured}$ (N)	$F_{t\_predicted}$ (N)	F_{t_error} (%)	$F_{f\_measured}$ (N)	$F_{f\_predicted}$ (N)	F_{f_error} (%)
1	60	0.051				259		7.7
2	80	0.051	336, 341,361	(352, 9.67)	4.7, 3.2, 2.5	263	(279, 6.7)	5
3	100	0.051				297		6
4	60	0.076	472, 475	(475 ,14.2)	0.6	348	(360, 9.9)	3.5
5	100	0.076	462		2	376, 382		4.2, 5.7
6	60	0.102	583		1.7	419, 426		3.3, 1.6
7	80	0.102	605	(593,19)	2		(433, 13.2)	
8	100	0.102	567		4.5	463		6.5

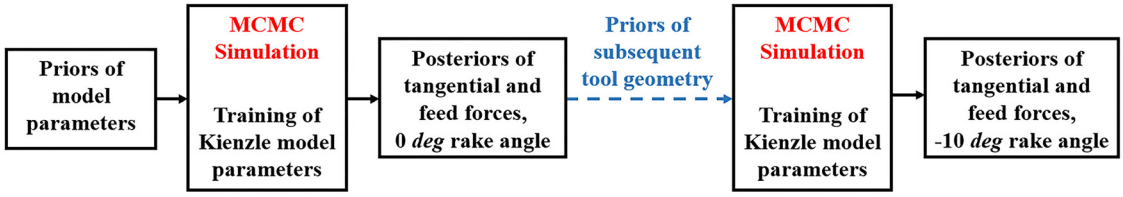

Fig. 18 Sequential training and prediction of cutting forces using Bayesian updating for different tool rake angles

(1) The prior mean and standard deviation values of K_{tt} and c_{tt} parameters, for −10 deg rake tool, are taken to be equal to the posterior of the previous geometry.
(2) The prior mean values of K_{ff} and c_f parameters, for −10 deg rake tool, are again taken to be equal to the posterior mean values of the previous geometry.
(3) The prior standard deviations of K_{ff} and c_f parameters, for −10 deg rake tool, are taken to be equal to the priors of the 0 deg rake tool, 140 MPa, and 0.025.

The above-mentioned approach for establishing of the prior's standard deviations denotes that allocating larger uncertainty on the prior values (i.e., less confidence in the prior knowledge) enables the simulation to rely more on the measurements. If more weight is given to the experiments, the parameters follow the likelihood function. On the other hand, defining smaller uncertainty on the prior distributions (more informative prior knowledge) refers that the simulation relies more on the prior. Based on this argument, it was decided to allocate smaller uncertainties to the tangential force model parameters (due to the more informative priors) and larger ones to the feed force model parameters.

Functional forms of the prior mean values, two standard deviation (2σ) uncertainty intervals, and the training force data points are shown in Fig. 19. According to the figure, the prior mean function of the tangential force approximates the training force data better than prior mean function of the feed force and both underestimate the data.

Once again, $N = 10{,}000$ samples were drawn from the proposal normal distributions, $q(K_{tt},c_t)$ and $q(K_{ff},c_f)$, and 1500 samples were considered as the burn-in period. The covariance matrices of the proposal distributions were tuned, so that the acceptance rate values of 45% and 39% were obtained for the drawn samples of the tangential and feed model parameters, respectively. Figure 20 shows the bivariate posterior distributions of K_{tt} and c_t and K_{ff} and c_f after one and two force updates, respectively. For the tangential force component, the mean values of K_{tt} and c_t are1658 MPa, and 0.27 and the standard deviations are 70 MPa and 0.017. For the feed force component, the mean values of K_{ff} and c_f, are 1255 MPa and 0.39 and the standard deviations are 72 MPa and 0.021. Comparing the posterior and prior joint distributions, it is seen that the uncertainties are reduced after updating. Additionally, the correlation

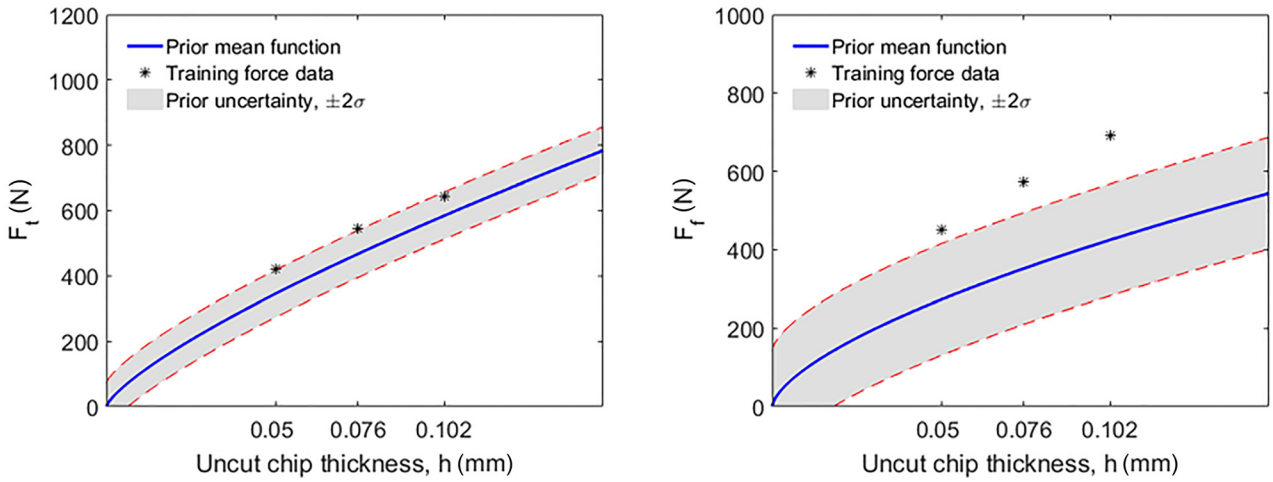

Fig. 19 Prior functions of the tangential forces (left) and feed force (right) with $\pm 2\sigma$ standard deviation uncertainty intervals for the tool rake angle −10 deg

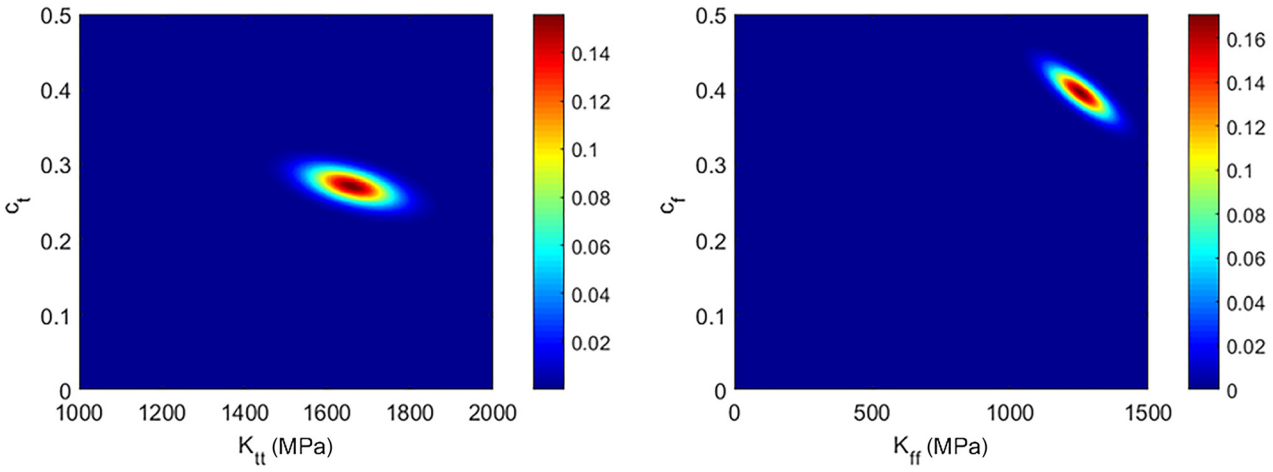

Fig. 20 Joint posterior distributions of K_{tt} and c_{tt} (left), and K_{ff} and c_f (right) for the tool rake angle −10 deg

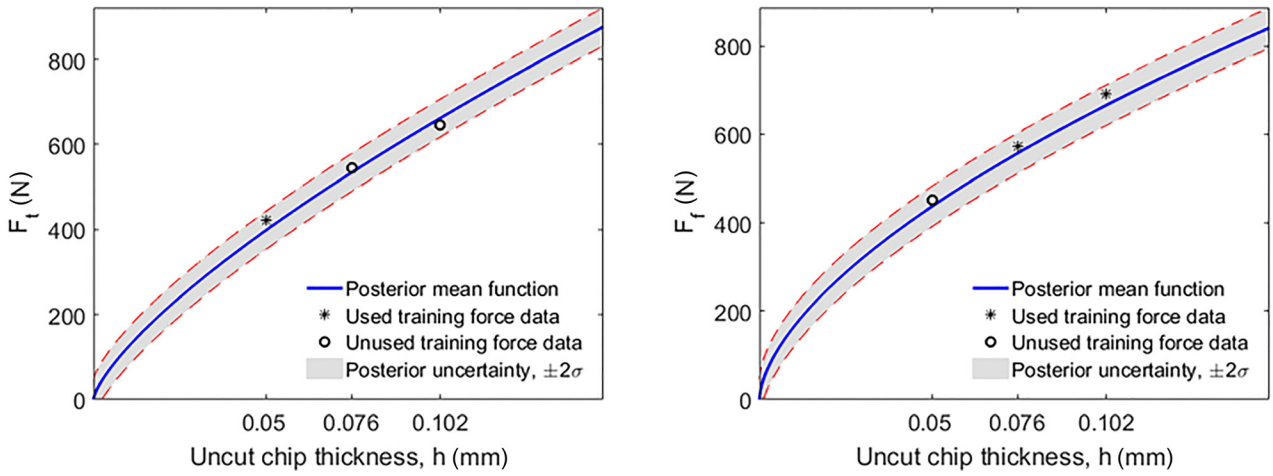

Fig. 21 Posterior functions of tangential (left) and feed (right) forces with $\pm 2\sigma$ standard deviation uncertainty intervals for the tool rake angle −10 deg

coefficient of the model parameters were calculated to be −0.53 for (K_{tt},c_t) and −0.80 for (K_{ff},c_f) joint distributions.

6.2 Cutting Force Prediction. Posterior force prediction was performed using the posterior distributions of K_{tt} and c_t and K_{ff} and c_f for Eqs. (7) and (8). Figure 21 shows the functional form of the posterior tangential and feed forces with the mean and standard deviation of 2σ. The regression fit parameters are $R^2 = 0.96$ (tangential force), and $R^2 = 0.965$ (feed force). The posterior of the tangential force was achieved using only one update due to the

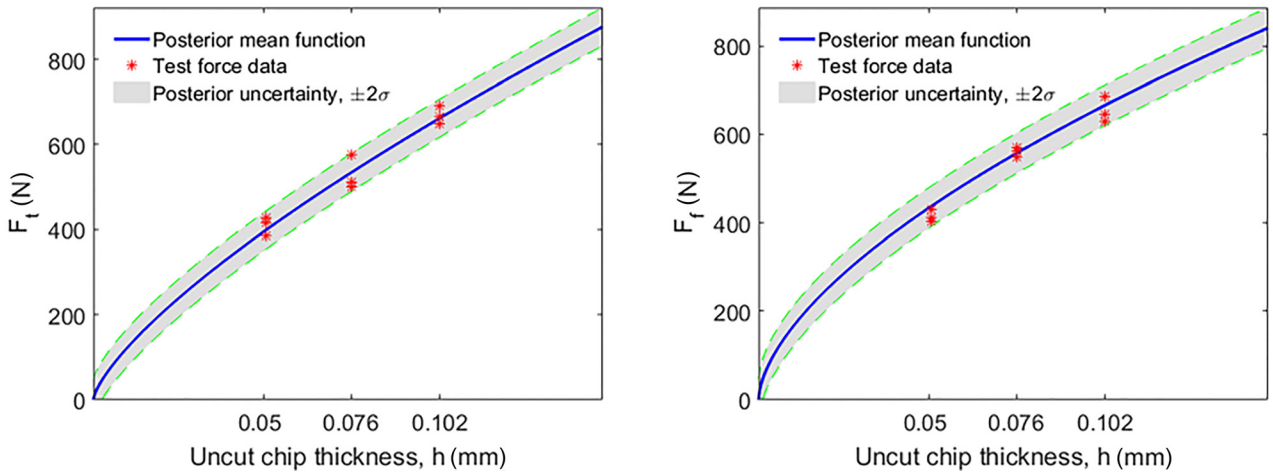

Fig. 22 Posterior functions for prediction of tangential (left) and feed (right) forces with $\pm 2\sigma$ standard deviation uncertainty intervals for the tool rake angle −10 deg

Table 2 Measured and predicted forces, and the corresponding percentage error using −10 deg rake angle tool

No.	V_c (m/min)	f (mm/rev)	$F_{t\_measured}$ (N)	$F_{t\_predicted}$ (N)	F_{t_error} (%)	$F_{f\_measured}$ (N)	$F_{f\_predicted}$ (N)	F_{f_error} (%)
1	60	0.051	427		6.5	430		1.8
2	80	0.051	415	(399, 8)	3.8		(438, 8.2)	
3	100	0.051	386		3	404, 411		8.5, 6.5
4	60	0.076	576	(534, 11.8)	7.2	571	(557, 12.2)	2.5
5	80	0.076	500, 514		6.8, 3.8	549, 562		1.5, 0.8
6	80	0.102	654	(662, 15.7)	1.2	629, 646, 686	(666, 16.2)	6, 3, 3
7	100	0.102	666, 691		0.6, 4			

more informative prior. This demonstrates the effectiveness of Bayesian inference as compared to least squares curve fitting, which requires at least two data points for the parameter identification, in this case. On the other hand, the posterior of feed force was obtained after two updates due to its less informative prior. According to the figures, the posterior mean functions accurately represent the training forces in tangential and feed directions.

Figure 22 illustrates the prediction of the tangential and feed test forces using the posterior functions. As can be seen, all the force data appear within the uncertainty intervals. Table 2 lists the experimental force values and the predicted mean tangential and feed forces with two standard deviation (2σ) uncertainty intervals for the −10 deg tool rake angle. Once more, the percent error between the measured and predicted mean forces were calculated and reported in the table. The maximum prediction error for the tangential force was calculated to be 7% and for the feed force was obtained to be 9%. This implies that the model parameters identification and forces prediction were performed with a good degree of accuracy using MCMC method applied to the Kienzle force model.

7 Conclusions

In this research, cutting forces prediction was performed using Bayesian inference (MCMC simulation) for the Merchant and Kienzle force models. The Mechanistic Merchant model is based on an assumption that the tool edge radius is zero, whereas the Kienzle force model takes into account the effect of cutting edge radius on specific cutting force coefficient. The results of the probabilistic force predictions using Merchant and Kienzle models for a 0 deg rake angle tool were obtained and discussed. Sequential force prediction was carried out by using the posterior probabilities of the Kienzle force model parameters for the 0 deg rake tool as the prior probabilities for the −10 deg rake tool. The main conclusions are summarized as following:

(1) The Kienzle force model predicted the tangential and feed cutting forces, successfully, while the Merchant model could not. The reason is that the Kienzle model can consider the size effect phenomenon in turning process. This refers to the nonlinearity due to the increase of the specific cutting energy with the reduced uncut chip thickness or increase of tool edge radius.
(2) The Kienzle posterior functions could predict the tangential and feed forces with the good degree of accuracy for both tool geometries. Using the 0 deg rake angle tool, the maximum prediction error values were reported 5% for the tangential force and 8% for the feed force. Using the 10 deg rake angle tool, the maximum errors of 7% for the tangential force and 9% for the feed force were obtained.
(3) The posterior functions of the tangential force components for both geometries were obtained using only one updating process, which is impossible in the case of parameter determination by least squares curve fitting. The uncertainty of the initial belief was reduced after updating in all instances. This suggests that Bayesian inference offers a preferred approach to force modeling by incorporating the minimal input and predicting forces under inherent uncertainties.

The result of the study can be further used to investigate the effect of cutting tools geometry and material on cutting force using Bayesian inference. The sequential probabilistic technique allows to incorporate historical knowledge about process parameters into the current simulation, so that the number of experiments is reduced.

Acknowledgment

The corresponding author gratefully acknowledges the "abroad research stays" grant of Karlsruhe House of Young Scientists (KYHS), spent for research period in the University of North Carolina at Charlotte.

References

[1] Merchant, M. E., 1945, "Mechanics of the Metal Cutting Process—II: Plasticity Conditions in Orthogonal Cutting," J. Appl. Phys., **16**(6), pp. 318–324.
[2] Shamoto, E., and Altıntas, Y., 1999, "Prediction of Shear Angle in Oblique Cutting With Maximum Shear Stress and Minimum Energy Principles," J. Manuf. Sci. Eng. **121**(3), pp. 399–407.
[3] Smithey, D. W., Kapoor, S. G., and DeVor, R. E., 2001, "A New Mechanistic Model for Predicting Worn Tool Cutting Forces," Mach. Sci. Technol., **5**(1), pp. 23–42.
[4] Schmitz, T. L., Smith, K. S., and Dynamics, M., 2009, "Milling Dynamics," *Milling*, Springer US, Boston, MA.
[5] Karandikar, J. M., 2013, *The Fundamental Application of Decision Analysis to Manufacturing*, University of North Carolina at Charlotte, Charlotte, NC.
[6] Karandikar, J. M., Abbas, A. E., and Schmitz, T. L., 2014, "Tool Life Prediction Using Bayesian Updating. Part 1: Milling Tool Life Model Using a Discrete Grid Method," Precis. Eng., **38**(1), pp. 9–17.
[7] Karandikar, J. M., Abbas, A. E., and Schmitz, T. L., 2014, "Tool Life Prediction Using Bayesian Updating. Part 2: Turning Tool Life Using a Markov Chain Monte Carlo Approach," Precis. Eng., **38**(1), pp. 18–27.
[8] Metropolis, N., Rosenbluth, A. W., Rosenbluth, M. N., Teller, A. H., and Teller, E., 1953, "Equation of State Calculations by Fast Computing Machines," J. Chem. Phys., **21**(6), pp. 1087–1092.
[9] Niaki, A. F., Ulutan, D., and Mears, L., 2016, "Parameter Inference Under Uncertainty in End-Milling γ'-Strengthened Difficult-to-Machine Alloy," ASME J. Manuf. Sci. Eng., **138**(6), p. 061014.
[10] Niaki, F. A., Ulutan, D., and Mears, L., 2015, "Parameter Estimation Using Markov Chain Monte Carlo Method in Mechanistic Modeling of Tool Wear During Milling," ASME Paper No. MSEC2015-9357.
[11] Gözü, E., and Karpat, Y., 2017, "Uncertainty Analysis of Force Coefficients During Micromilling of Titanium Alloy," Int. J. Adv. Manuf. Technol., **93**(1–4), pp. 839–855.
[12] Schmitz, T. L., Karandikar, J., Ho Kim, N., and Abbas, A., 2011, "Uncertainty in Machining: Workshop Summary and Contributions," ASME J. Manuf. Sci. Eng., **133**(5), p. 051009.
[13] Mehta, P., Kuttolamadom, M., and Mears, L., 2017, "Mechanistic Force Model for Machining Process—Theory and Application of Bayesian Inference," Int. J. Adv. Manuf. Technol., **91**(9–12), pp. 3673–3682.
[14] Weber, M., Hochrainer, T., Gumbsch, P., Autenrieth, H., Delonnoy, L., Schulze, V., Löhe, D., Kotschenreuther, J., and Fleischer, J., 2007, "Investigation of Size-Effects in Machining With Geometrically Defined Cutting Edges," Mach. Sci. Technol., **11**(4), pp. 447–473.
[15] Vollertsen, F., Biermann, D., Hansen, H. N., Jawahir, I. S., and Kuzman, K., 2009, "Size Effects in Manufacturing of Metallic Components," CIRP Ann.-Manuf. Technol., **58**(2), pp. 566–587.
[16] Altintas, Y., and Ber, A., 2001, *Manufacturing Automation: Metal Cutting Mechanics, Machine Tool Vibrations, and CNC Design*, Cambridge University Press, Cambridge, UK.
[17] Klocke, F., Adams, O., Auerbach, T., Gierlings, S., Kamps, S., Rekers, S., Veselovac, D., Eckstein, M., Kirchheim, A., Blattner, M., Thiel, R., and Kohler, D., 2015, "New Concepts of Force Measurement Systems for Specific Machining Processes in Aeronautic Industry," CIRP J. Manuf. Sci. Technol., **9**, pp. 31–38.

[18] Andrieu, C., De Freitas, N., Doucet, A., and Jordan, M. I., 2003, "An Introduction to MCMC for Machine Learning," Mach. Learn., **50**(1/2), pp. 5–43.
[19] Roberts, G. O., and Rosenthal, J. S., 2001, "Optimal Scaling for Various Metropolis-Hastings Algorithms," Stat. Sci., **16**(4), pp. 351–367.
[20] Hoff, P. D., 2009, *A First Course in Bayesian Statistical Methods*, Springer, New York.
[21] Niaki, F. A., 2016, *A Probabilistic-Based Approach to Monitoring Tool Wear State and Assessing Its Effect on Workpiece Quality in Nickel-Based Alloys*, Clemson University, Clemson, SC.
[22] Geweke, J., 1992, "Evaluating the Accuracy of Sampling-Based Approaches to the Calculation of Posterior Moments," Bayesian Stat., **4**, pp. 169–193.
[23] Schimmel, R. J., Endres, W. J., and Stevenson, R., 2002, "Application of an Internally Consistent Material Model to Determine the Effect of Tool Edge Geometry in Orthogonal Machining," ASME J. Manuf. Sci. Eng., **124**(3), p. 536.
[24] Denkena, B., and Tönshoff, H. K., 2011, *Spanen: Grundlagen*, Springer, Berlin.